

Nature of Dark Energy and Polarization Measurements

R. Mainini¹, L.P.L. Colombo² & S.A. Bonometto³

*Physics Department G. Occhialini, Università degli Studi di Milano–Bicocca,
Piazza della Scienza 3, I20126 Milano (Italy)*

I.N.F.N., Via Celoria 16, I20133 Milano (Italy)

Abstract

We discuss at which noise level measures of polarization on wide angular scales, together with anisotropy data, can fix DE parameters. Anisotropy–polarization correlations, at low l , for RP models, are peculiar and similar to open models. Using a likelihood analysis, we show then that it can be possible to distinguish models with DE due to RP potentials from Λ CDM and other quintessence models, already with a pixel noise similar to the one MAP grants for anisotropy. This noise level may be not so far from the one achieved by the SPORt experiment on polarization. On the contrary, fixing the energy scale Λ for RP potentials or distinguishing between Λ CDM and other quintessence potentials requires a much lower pixel noise, that no planned polarization experiment is still able to achieve.

Key words: Cosmic Microwave Background, Cosmology: Cosmological Parameters
PACS: 98.70.Vc, 98.80.-k

1 Introduction

The nature of DE is one of the main puzzles of modern cosmology. DE was first required by SNIa data (see, e.g., Perlmutter et al 1998, Riess et al 1998), that indicate an accelerated cosmic expansion. A joint analysis of CMB and LSS observations (see, e.g., Percival et al. 2002, Efstathiou et al 2002) also favors a flat Universe with $\Omega_m \simeq 0.3$ and $\Omega_b h^2 \simeq 0.02$ ($\Omega_{m,b}$: matter and baryon density parameters; h : Hubble parameter in units of 100 km/s/Mpc).

¹ E-mail: roberto.mainini@mib.infn.it

² E-mail: loris.colombo@mib.infn.it

³ E-mail: silvio.bonometto@mib.infn.it

The residual energy content of the world, in the present epoch, should not be observable in the number-of-particle representation.

Much attention has been devoted to the idea that such energy arises from false vacuum, whose pressure p_{DE} and energy density ρ_{DE} have ratio $w = -1$. The main problem is that, in this case, ρ_{DE} is a minute fraction ($\sim 10^{-50}$) of vacuum energy density before the electroweak phase transition and this implies a extremely fine tuning on energy after such transition.

Another appealing possibility, apparently reducing fine tuning requirements, is that DE is the energy of a self-interacting scalar field ϕ (*quintessence*; see, e.g., Ratra-Peebles 1988, RP hereafter; Wetterich 1995; Ferreira & Joyce 1998; Perrotta & Baccigalupi 1999; Steinhardt et al. 1999; Zlatev et al. 1999; Albrecht & Skordis 2000; Amendola 2000; Brax, Martin & Riazuelo 2000). Then

$$\rho_{DE} = \frac{\dot{\phi}^2}{2a^2} + V(\phi) \quad , \quad p_{DE} = \frac{\dot{\phi}^2}{2a^2} - V(\phi), \quad (1.2)$$

$V(\phi)$ being the self-interaction potential, and w becomes negative, eventually approaching -1, as soon as the kinetic term $\rho_k = \dot{\phi}^2/(2a^2)$ becomes smaller than the potential V . In order to work out how w varies in time, Friedmann equations, in association with the equation of motion of ϕ , ought to be integrated and integrals depend on the form of V . Quintessence models are close to Λ CDM when the potential term dominates. When w approaches -1/3, instead, their behavior is close to open CDM models.

In principle, there is a large arbitrariness on self-interaction potentials. However, among potentials admitting a *tracking* solution, a particular relevance is kept by RP and SUGRA (Brax & Martin 1999, 2000) expressions:

$$V(\phi) = \Lambda^{4+\alpha}/\phi^\alpha \quad , \quad V(\phi) = (\Lambda^{4+\alpha}/\phi^\alpha) \exp(\kappa\phi^2/2) \quad . \quad (1.1)$$

Here Λ is an energy scale (not the cosmological constant), currently set in the interval 10^2 – 10^{10} GeV, ranging between the electroweak scale and the scale at which the soft breaking of supersymmetries is though to have occurred. The potentials (1.1) depend also on the exponent α ; fixing Λ and α , the DE density parameter Ω_{DE} is set. Here we use Λ and Ω_{DE} as free parameters, α being derived from them; in SUGRA potentials, $\kappa = 8\pi G$ (G : gravitational constant).

From the observational point of view, distinguishing between Λ CDM and quintessence models is not easy. Going farther, to detect the shape of the potential V , is an even tougher duty. Here we shall debate the imprints that the shape of V left on CMB (cosmic microwave background) spectra and discuss how far anisotropy and polarization measurements, on the large angular scales, may constrain V . If favorable (but not exceptional) conditions are given, polarization measures, at a sensitivity level not far from experiments

in progress, will be shown to be able to provide significant information, possibly *excluding* that a RP potential describes cosmic DE. We shall do so by using a detailed likelihood analysis, assuming that polarization measures come from an experiment similar to the Sky Polarization Observatory (SPOrt: see, e.g., Macculi et al, 2000; Carretti et al, 2000; Peverini et al, 2001), but with noise levels lower (but not much lower) than these authors claim to be able to achieve. On the contrary, we shall see that, to confirm that DE comes from a RP potential (or from any other potential), a much higher sensitivity is required. Our results, however, are not directly related to the above experiment and can be easily extrapolated to other observational contexts.

2 The cosmic opacity to CMB photons

Large angle polarization spectra are highly dependent on the cosmic opacity to CMB photons. In the present cosmic epoch, although diffuse baryonic materials are almost completely ionized, the scattering time for CMB photons $t_s \simeq 4.45 \cdot 10^{18} \Omega_b^{-1} h^{-2} \text{s}$ (h : Hubble parameter in units of 100 km/s/Mpc) exceeds the Hubble time $t_H = 3.09 \cdot 10^{17} h^{-1} \text{s}$ and the Universe is transparent to CMB photons. These figures can be extrapolated to the past, but, while $t_s \propto a^3$ (a : the scale factor), the dependence of t_H on a depends on the cosmological model. In an expansion regime dominated by non-relativistic matter, a fully ionized Universe is opaque to CMB at $z > z_{op} \simeq 5 (\Omega_b h^2)^{-2/3}$. Therefore, assuming $\Omega_b h^2 \leq 0.022$ (standard BBNS limits; see, e.g., Dolgov 2002 for a recent review) and $h \simeq 0.5\text{--}0.7$, we have $z_{op} > 64$, safely above the expected reionization redshift z_{ri} . No reasonable cosmological model allows a substantial reduction of such z_{op} .

On the contrary, the precise value of the optical depth $\tau (\ll 1)$, does depend on the model and, in particular, on z_{ri} . Recent data on high- z QSO's (Djorgovski et al. 2001; Becker et al. 2001) indicate that at least a fraction of neutral hydrogen is present, in the intergalactic medium, at $z \gtrsim 6$. These very authors, however, warn the reader against an immediate conclusion that $z_{ri} \simeq 6$. Reionization can be a slow and/or patchy process and primeval object formation can be consistent both with an effective $z_{ri} \simeq 6$ or a significantly greater value. In Fig. 1 we show how τ is related to z_{ri} and model parameters, considering a wide set of cosmological models. For $z_{ri} \lesssim 15$, values of τ up to $\sim 0.15\text{--}0.20$ are licit.

CMB anisotropy data provide no significant constraint to τ ; the most stringent constraint comes from the analysis of recent balloon data (Stompor et al 2002) and amounts to requiring $\tau < 0.40$, at the $2\text{-}\sigma$ level. Such loose limits arise because of the degeneracy between τ and n (primeval spectral index), in anisotropy data analysis. In a recent paper (Colombo & Bonometto, 2002)

we discussed how much such degeneracy can be removed using polarization measures. Recent observations (Kovac et al. 2002) confirm that the CMB is polarized, but the sensitivity level of experiments ought to be significantly increased before that polarization measures can allow to reduce the above $n-\tau$ degeneracy.

A recent analysis, taking into account all sorts of constraints (Miralda-Escudé 2002) and consistently with the above discussion, concludes that the value of τ is likely to fall in the interval 0.04–0.08; this is the interval that we shall explore here below.

3 CMB angular spectra

A first insight into the detectability of a potential is given by the expected shape of angular spectra C_l^A ; $A = T, E, B, X$ stand for anisotropy, E - and B -mode polarization and anisotropy–polarization (TE) cross correlation; only E -mode polarization is considered through this paper. In Fig. 2–5 we show the shapes of $C_l^{T,X,E}$ when the potential is RP or SUGRA, τ is 0.04 or 0.08, for various values of the energy scale Λ . Such spectra are obtained with a suitable extension of the public program CMBFAST⁴.

Figs. 2 to 5 show that the main dependence on the nature of DE and, in particular, on the energy scale Λ , both for RP and SUGRA models, is concentrated in low- l TE correlation spectra. In particular, Figs. 2 and 3 show that C_l^X is negative, at low l , for RP potentials, while, in SUGRA models, such feature is absent. Quite in general, negative C_l^X are not an exceptional feature: all models yield alternate intervals of positive and negative C_l^X as l increases. In most spatially flat models, however, the C_l^X spectrum, at low l values, starts from positive values. On the contrary, open CDM models, with a significant τ , yield a C_l^X spectrum starting from negative values.

In the discussion section, we shall show that RP models share precise features with open models. The critical point is the actual dependence of ρ_{DE} on the scale factor a . In Λ CDM models, ρ_{DE} does not depend on a . In open model, the relevance of the curvature term decreases with a^{-2} . If the energy density of the scalar field ϕ , yielding DE, scales with a law close to a^{-2} , the C_l^X spectrum can start from negative values. On the contrary, when such scaling is closer to Λ CDM, such negative components are absent.

Setting a border between these behaviors is not an easy task, also because the a dependence of ρ_{DE} , for a generic potential V , is not a simple power law.

⁴ <http://physics.nyu.edu/matiasz/CMBFAST/cmbfast.html>

Accordingly, the results given in this paper concern specific potential classes.

4 Likelihood analysis

Model likelihood is determined in respect to possible results of anisotropy and polarization measurements, obtained through definite observational apparatus, for specific cosmological models. In particular, polarization data sets are built with reference to the features of the SPOrt experiment.

At variance from other space experiments (MAP and PLANCK), SPOrt has been explicitly designed to measure the Stokes parameters Q and U and to minimize systematics and instrumental polarization. SPOrt will observe a sky area with declination $|\delta| \leq 51.6^\circ$ ($\sim 80\%$ of the whole sky). The lifetime of the experiment will be at least 1.5 years, but an extension is not unlikely; data will be binned in a number of pixels ranging from 662 to several thousands, depending on the effective duration of the flight and efficiency.

Here we assume that pixels are distributed according to the HEALPix⁵ package, with $N^{side} = 16$, and smoothed with a Gaussian beam of FWHM of 7° . We therefore have, on the whole sky, 3072 pixels, whose centers lie at an average angular distance of $\sim 3.7^\circ$. Once polar caps are excluded, there remain 2448 pixels, providing measures of the Stokes parameters Q and U .

SPOrt polarimeters will provide no anisotropy data. Such information will be however available through other experiments (COBE, MAP) and we assume here that no peculiar problem arises in correlating SPOrt and anisotropy data. Of course, anisotropy data probe a different sky area, i.e. the whole sky, excluding the area with declination $|\delta| < 20^\circ$, where galactic contamination is severe. (On the contrary, such contamination can be assumed to be under control, for polarization data; see, e.g., Bruscoli et al. 2002; Tucci et al. 2002.) In this sky area there are 1984 pixels. For 1360 of them, both anisotropy and polarization data are supposed to be available.

Random noise (σ_{pix}^P) is included in artificial data, assuming it to be uncorrelated, both among pixels and between Q and U , in the case of polarization measures. We assume $\sigma_{pix}^T = 1 \mu\text{K}$ for temperature data (as expected for MAP measurements, extended to 4 years, scaled to the SPOrt resolution). On the contrary, one of the main variables we consider is the noise level for polarization data.

At present, the SPOrt experiment team claims to be able to achieve a noise

⁵ <http://www.eso.org/science/healpix/>

level $\sigma_{pix}^P \simeq 5.3 \frac{N_{side}}{8} \sqrt{\frac{1.5}{\lambda} \frac{0.5}{\epsilon}} \mu\text{K}$ per pixel, where λ is the experiment's lifetime in years while ϵ indicates the detection efficiency. Our analysis considers σ_{pix}^P 's in the interval comprised from 0.1 to 1 μK per pixel. Even at its highest value, such noise is smaller than the expected experimental figures. In order to achieve it, substantial improvements in apparati and/or long lifetime extensions are needed.

Dealing with low l 's, cosmic variance must be carefully taken into account. We explore this point by simulating and analyzing a large number of artificial data sets. Results will be both synthesized into average predictions and analyzed providing the frequency of possible determinations.

In order to maximize the ability of an experiment to determine the energy scale Λ , we assume that most other model parameters are known from other experiments. In this analysis we take $\Omega_{DE} = 0.7$, $\Omega_b h^2 = 0.02$, $h = 0.7$ and a primeval spectral index $n = 1$. We considered also different values for these parameters, but the likelihood distributions are essentially independent from them. On the contrary, such distributions depend on the choice of τ ; we therefore studied likelihood distributions for $\tau = 0.04$ and 0.08.

We report first results for RP models, considering the 3 energy scales: $\Lambda/\text{GeV} = 10^3$, 10^6 , 10^9 . In Figs. 6 to 8 we show the average likelihood distributions for such models.

In Figs. 9 to 11, we report the distributions of the 1–2–3 σ lower limits on Λ , for $\tau = 0.04$ and 0.08, $\Lambda = 10^3$ and 10^6 , $\sigma_{pix}^P = 0.1 \mu\text{K}$ and $1 \mu\text{K}$.

It should be outlined that cosmic acceleration is granted by RP models only if $\Lambda \lesssim 10^4 \text{GeV}$, while RP models with $\Lambda > 10^6 \text{GeV}$ are inconsistent with SNIa data (2- σ level). On the contrary, $\Lambda < 1 \text{GeV}$, besides of being physically unattractive, yield spectra indistinguishable from ΛCDM . Hence, when a lower limit on Λ lies below 1 GeV, this means that the model is indistinguishable from ΛCDM .

Fig. 12 is analogous to Fig. 6, but concerns a SUGRA model with $\Lambda = 10^9 \text{GeV}$ and $\tau = 0.08$; among the cases considered here, this is the one which allows the best recovery of Λ . In Fig. 13, we report distributions of 1 σ lower limits on Λ for such model.

Although unlikely to be achieved by the SPOrt experiment, a noise level $\sim \sigma_{pix}^P = 1 \mu\text{K}$ can be considered a reasonable achievements with available technologies. We can resume the results shown in the above figures by saying that, not only at such noise level, but also reducing noise by a factor 10, the energy scale Λ cannot be detected for SUGRA models, at least with large angular scale experiments. The situation is much better for RP models. There is a substantial fraction of realizations of the model with $\Lambda = 10^6 \text{GeV}$ and

$\tau = 0.08$ which can be distinguished from Λ CDM, even at the $3\text{-}\sigma$ level. At the $2\text{-}\sigma$ level such model could be confused with Λ CDM only in quite a small fraction of realizations. But also models with $\Lambda = 10^3 \text{GeV}$ and/or $\tau = 0.04 \mu\text{K}$ can be distinguished from Λ CDM in a substantial fraction of realizations, at least at the $2\text{-}\sigma$ level. However, if we aim farther and wish to determine Λ , we notice that, even reducing the noise level by a factor 10, its order of magnitude meets a fair lower limit in less than 10% of cases (3σ level).

5 Discussion

Let us first discuss how the likelihood distribution can be obtained from the spectra of a given model, taking into account that the number of pixels for anisotropy and polarization (N_T and N_P) in our (artificial) data are however different. Let then T_j be the anisotropy measured in N_T pixels and Q_j and U_j the Stokes parameters measured in N_P pixels. In general, let us define vectors $\mathbf{x} \equiv (T_1, \dots, T_{N_T}, Q_1, \dots, Q_{N_P}, U_1, \dots, U_{N_P})$, of $N_s = N_T + 2N_P$ components, defining an observed state of anisotropy and polarization. Once a Λ value is assigned, the angular spectra $C_l^A = (C_l^T, C_l^E, C_l^X)$ are univocally determined. On the contrary, a data vector \mathbf{d} , of N_s components, built from them, is just a *realization* of such model: once the N_s component vector \mathbf{d} is assigned, the value of Λ is not univocally fixed.

A function

$$L(\mathbf{d}|C_l^A) \propto [\det \mathbf{M}]^{-\frac{1}{2}} \exp\left[-\frac{1}{2}\mathbf{d}^T \mathbf{M}^{-1} \mathbf{d}\right] \quad (5.1)$$

is then built, to yield the likelihood of a given set of C_l^A (i.e., of a given Λ value), if \mathbf{d} is observed. The main ingredient of L is the correlation matrix $\mathbf{M}_{ij} = \langle \mathbf{x}_i^T \mathbf{x}_j \rangle = \mathbf{S}_{ij} + \mathbf{N}_{ij}$; here \mathbf{S}_{ij} is the signal term and \mathbf{N}_{ij} is due to the noise. The components \mathbf{M}_{ij} yield the correlation between the i th and j th elements of data vectors \mathbf{x} corresponding to particular choices of C_l^A , i.e. of Λ values. The construction of the (model dependent) signal term, however, does not require to build explicitly the vectors \mathbf{x} . The procedure to be followed, in the case when both anisotropy and polarization data are available, is explicitly reported by Zaldarriaga (1998). The construction of the noise term is simpler, as we expect no noise correlation, and the matrix $\mathbf{N}_{ij} = \delta_{ij} \sigma_{T,pix}^2$ (for $i = 1, \dots, N_T$) and $\mathbf{N}_{ij} = \delta_{ij} \sigma_{P,pix}^2$ (for $i = N_T + 1, \dots, N_s$) is diagonal.

In what follows, the technical role of the C_l^A spectra does not need to be further outlined and the likelihood function is explicitly considered to depend on Λ . In particular, we assume that the most probable Λ value, for a given anisotropy–polarization state \mathbf{d} , is the one which maximizes the likelihood. By integrating the likelihood distribution along the Λ axis, we are then able to find the intervals corresponding to 1–2–3 σ levels.

In order to explore cosmic variance, 1000 realizations of each model were considered; the likelihood curves plotted in the Figs. 6–7–8–12 are averages of the results of such realizations. 1–2–3 σ value distributions, instead, allow to appreciate the spread among the results of each such realization.

The feature which explains why RP model likelihoods can enable us to distinguish them from Λ CDM, in several cases, is the negative TE correlation at low l . In the case of SUGRA models such TE anticorrelation is absent and large angle data seem unsuitable to provide information on DE nature.

Negative TE correlations are essentially related to the simultaneous action of ISW effect and cosmic opacity. The former effect is a consequence of the varying rate of expansion, when we pass from matter to curvature dominance, in open models, or from matter to vacuum dominance in Λ CDM models. However, while the former kind of passage, in the presence of cosmic opacity, does produce anticorrelation, the latter kind of passage does not.

The capacity of RP models to induce anticorrelation, as we shall see, is related to their features, which more closely approach open CDM, rather than Λ CDM. The opposite is true for SUGRA models.

A full understanding of model dynamics requires that the whole set of Boltzmann equations, describing photon distribution, is followed in time. Such equations are shown in a number of papers, together with equations ruling the dynamics of fluctuations in other components of a model (see, e.g., Ma & Bertschinger 1995). Signs and other definitions that we adopt here are the same as in the public code CMBFAST. Let us then indicate by $F_l(k, t)$ and $G_l(k, t)$ the Boltzmann components for anisotropy and polarization, respectively, k and t being the wave-number and conformal time.

Let us report here the set of equations fulfilled by the G_l components in spatially flat models:

$$\dot{G}_l = a n_e \sigma_T \left[-G_l + \frac{\Pi}{2} \left(\delta_{l0} + \frac{\delta_{l2}}{5} \right) \right] + \frac{k}{2l+1} [l G_{l-1} - (l+1) G_{l+1}] \quad (5.2f)$$

(δ_{ln} is the Kronecker symbol). Here a is the scale factor, n_e is the free electron density, σ_T is the Thomson cross-section. Here

$$\Pi = G_o + G_2 + F_2, \quad (5.3)$$

is the only vehicle transferring signals from anisotropy to polarization.

In a non-flat geometries eq. (5.2f) becomes

$$\dot{G}_l = a n_e \sigma_T \left[-G_l + \frac{\Pi}{2} \left(\delta_{l0} + \frac{\delta_{l2}}{5} \right) \right] + \frac{\beta}{2l+1} [l b_l G_{l-1} - (l+1) b_{l+1} G_{l+1}] ; \quad (5.2o)$$

here $\beta^2 = k^2 + K$ and $b_l^2 = 1 - Kl^2/\beta^2$, with $K = -(1 - \Omega_m)H_0^2$, H_0 being the present value of the Hubble parameter.

Let us recall that the opacity to CMB photons reads $\tau = \int_t^{t_o} n_e(t')\sigma_T a(t') dt'$. Accordingly, the damping coefficient, in front of the first term at the r.h.s. of eq. (5.2), is $-\dot{\tau}$. Quite in general, when n_e is large, all G_l are exponentially damped. On the contrary, when n_e is low, the polarization signal spreads along the G_l component series.

In order to produce polarization, therefore, there must however be a seed coming from anisotropy, linked to the non-vanishing of the quadrupole term $F_2(k, t)$. If $F_2(k, t)$ becomes significant only when n_e is low, little polarization is produced on harmonics with l corresponding to such k . It is so for wavelengths $2\pi/k$ entering the horizon well after recombination, which correspond to spectral components with $l \ll 200$, unless reionization occurs. This explains the sudden rise of C_l^P in Fig. 2–5, when $\tau > 0$ is considered.

Let F_l^o (G_l^o) be the value taken by F_l (G_l) at the present time t_o . In spatially flat models, the angular spectra read

$$C_l^T = \frac{\pi}{4} \int d^3k P_o(k) |F_l^o(k)|^2, \quad C_l^P = \frac{\pi}{4} \int d^3k P_o(k) |G_l^o(k)|^2,$$

$$C_l^X = \frac{\pi}{4} \int d^3k P_o(k) F_l^o(k) G_l^o(k), \quad (5.4f)$$

$P_o(k)$ being the primeval fluctuation spectrum. In open model, angular spectra expressions are slightly more complex and read

$$C_l^T = \frac{\pi}{4} \int d^3\beta P_o(q) |F_l^o(\beta)|^2, \quad C_l^P = \frac{\pi}{4} \int d^3\beta P_o(q) |G_l^o(\beta)|^2,$$

$$C_l^X = \frac{\pi}{4} \int d^3\beta P_o(q) F_l^o(\beta) G_l^o(\beta); \quad (5.4o)$$

here $q = (\beta^2 - 4K)^2/\beta(\beta^2 - K)$. Clearly, for $\Omega_m = 1$, both β and q return k .

Both eqs. (5.2) and (5.4) indicate the presence of suitable shifts in the k -space, when open models are considered. In particular, the b_l coefficients in eq. (5.2o) are responsible for the shifts of C_l peaks, while the shifts due to the passage from k to β and q , in eq. (5.4o), displace the power of the spectrum P_o through the harmonics F_l at small l , i.e. on scales comparable with the curvature scale.

Apart of these geometric and power shifts, the main difference between flat and open models resides in the equation fulfilled by the gravitational field fluctuations \dot{h} and $\dot{\eta}$. In the synchronous gauge, for open models:

$$2\bar{k}^2\dot{\eta} = 8\pi G a^2 \left[\sum_c (\rho_c + p_c)\theta_c - \dot{h}_{\rho_o,cr}(1 - \Omega_m)/a^2 \right]; \quad (5.5o)$$

here $\rho_{o,cr}$ being the critical density at $z = 0$ and \sum_c indicates a sum over all (relativistic or non-relativistic) matter components. In the same gauge, for flat models with DE:

$$2k^2\dot{\eta} = 8\pi G a^2 \left[\sum_c (\rho_c + p_c)\theta_c + (\rho_{DE} + p_{DE})\theta_{DE} \right], \quad (5.5f)$$

where the DE term has been set in evidence, with its possible fluctuations. The wave-numbers \bar{k}^2 and k^2 are shifted by $3K$. Once again this corresponds to a shift in the k -space.

Let us notice soon that, in a Λ CDM model, no DE fluctuations exist and, furthermore, $\rho_{DE} = -p_{DE}$, so that the second term at the r.h.s. of eq. (5.5f) vanishes.

In models with dynamical DE, instead, θ_{DE} does not vanish and, in general, $\rho_{DE} \neq -p_{DE}$. Accordingly, the second term in square brackets in eq. (5.5f) may read $\theta_{DE}\rho_{o,cr}(1-\Omega_m)(1+w)(\rho_{DE}/\rho_{o,DE})$ (the ratio in the last parenthesis tells us how DE energy scales with a). This term is then analogous to the second term in square bracket in eq. (5.5o). It would coincide with it if $w = -1/3$ and, namely, if $\theta = -\dot{h}/2$. If the latter is true, we can expect that, apart of a different power distribution along the l axis and geometric effects at greater l , there can be specific similarities in the behavior of open and quintessence models.

The relation between $\dot{h}/2$ and θ_{DE} can be studied through the equation

$$\theta_{DE} + \frac{\dot{h}}{2} = -\frac{1}{1+w} \left[\dot{\delta}_{DE} + 3\frac{\dot{a}}{a}(c_s^2 - w)\delta_{DE} \right], \quad (5.6)$$

whose validity indicates that quintessence behaves as a fluid; here c_s is the sound velocity in quintessence. This equation can be derived from the equation of motion of ϕ , as shown in Appendix A. An order of magnitude estimate, however, tells us soon that $\theta_{DE} \sim k^2 t \delta_{DE}$; then, the ratio between θ_{DE} and the r.h.s. is $\sim (t/L)^2$, where L is the scale related to k . When $t \ll L$ (before horizon crossing), the θ_{DE} term is negligible, in comparison with the r.h.s.. For $L \ll t$ (after horizon crossing), the contrary is true. Hence, before horizon crossing, $\dot{h}/2$ is essentially required to equate the r.h.s. and, therefore, the ratio $-\dot{h}/2\theta_{DE}$ shall exceeds unity. At horizon crossing such ratio must approach unity and keep to such value as t grows greater than L .

This point can also be numerically inspected. In Fig. 14, the ratio $-\dot{h}/2\theta_{DE}$ is plotted against a , for those k values which yield the top contribution to the l harmonics indicated in the figure, in the case of a RP model. Clearly, about horizon crossing, θ_{DE} is already quite close to $-\dot{h}/2$.

The main differences between open and quintessence models, in the r.h.s. of

eqs. (5.5) are therefore relegated to times before horizon crossing. Afterwards, the residual difference is due to a factor $1+w$. If w is too close to -1 , however, such factor risks to spoil the similarities noticed hereabove.

The changes in $\dot{\eta}$ directly act on F_2 . The equation fulfilled by this spectral component reads:

$$\begin{aligned} \dot{F}_2(k, t) = a n_e \sigma_T \left[-F_2(k, t) + \frac{\Pi(k, t)}{10} \right] + \frac{k}{5} [2 F_1(k, t) - 3 F_3(k, t)] + \\ + \frac{8}{5} \left(\dot{\eta}(k, t) + \frac{\dot{h}(k, t)}{6} \right) \end{aligned} \quad (5.7f)$$

in flat models, while in open models we have:

$$\begin{aligned} \dot{F}_2(\beta, t) = a n_e \sigma_T \left[-F_2(\beta, t) + \frac{\Pi(\beta, t)}{10} \right] + \frac{\beta}{5} [2 b_2 F_1(\beta, t) - 3 b_3 F_3(\beta, t)] + \\ + \frac{8 \beta}{5 k} b_2 \left(\dot{\eta}(\beta, t) + \frac{\dot{h}(\beta, t)}{6} \right) . \end{aligned} \quad (5.7o)$$

Let us recall that F_2 is the only term of Π where anisotropy contributes. Such contribution is therefore directly affected by a change in the equation of the gravitational field, which describes the ISW effect in the synchronous gauge and can be similar in open models and in models with dynamical DE, provided that w is not too far from $-1/3$.

Accordingly, when open models show negative TE correlations at low l , we can expect the same to occur in flat RP models. On the contrary, SUGRA models, which grant a cosmic acceleration much closer to Λ CDM models, due to a w value not too far from -1 , should not be expected to give negative TE correlation and cannot be tested in the same way as RP models.

6 Conclusions

In this paper we showed that a particular class of dynamical DE models can be fairly safely *falsified* using large angle CMB polarization data. Models with DE due to a scalar field, self-interacting through a RP potential, belong to such class. In general, however, we expect that any model with dynamical DE, yielding a $w(= p_{DE}/\rho_{DE})$ value not too far from $-1/3$, can be tested through similar data.

In fact, an experiment able to detect CMB polarization with a noise level $\sim \sigma_{pix}^P = 1 \mu\text{K}$, as we considered in this analysis, can be considered a reasonable

achievements with available technologies. With reference to such noise, we have seen that there is a substantial fraction of realizations of a RP model with $\Lambda = 10^6 \text{GeV}$ and $\tau = 0.08$ which can be distinguished from ΛCDM , even at the $3\text{-}\sigma$ level. Of course, observers have access to a single realization of the true cosmological model. The above statement, therefore, indicates that the data analysis of a polarization experiment, with a noise level of $\sim \sigma_{pix}^P = 1 \mu\text{K}$, has, at least, $\sim 30\%$ of probabilities to indicate that the true model is RP, if this is true. At the $2\text{-}\sigma$ level, such model could be confused with ΛCDM only in quite a small fraction of realizations. But also RP models with $\Lambda = 10^3 \text{GeV}$ and/or $\tau = 0.04 \mu\text{K}$ are potentially distinguishable from ΛCDM in a significant fraction of realizations, at least at the $2\text{-}\sigma$ level.

The only planned polarization experiment aiming to large angle polarization data is SPOrt. The noise level that the SPOrt team claims to be able to attain is ~ 4 times greater than the worst level considered in this paper. However, other experiments, planned to provide data with greater resolution, can also provide large-angle harmonics. The sensitivity planned for SPOrt is however insufficient to compare RP models with data. On the contrary, if the MAP satellite, although not built to minimize systematic effects on polarization estimates, is able to provide polarization data with the same noise level expected for anisotropy data, a fair test of RP models will then be possible. Finally, with the sensitivity expected for PLANCK, RP and similar models can be surely tested.

It must be however clear that, in order to determine the energy scale Λ for RP potentials (let alone to distinguish between ΛCDM and other quintessence potentials) a much lower pixel noise is required. No planned polarization experiment will achieve such noise level soon and other observations will be hopefully able to fix such parameters with smaller experimental effort.

Acknowledgements – LC acknowledges the financial support of ASI, within the activities related to the SPOrt experiment. The CINECA consortium is thanked for making its facilities available for this work. The components of the SPOrt team are also thanked for discussions on the topics of this research. The public programs CMBFAST, by U. Seljak & M. Zaldarriaga, and HEALPix, by K.M. Górski et al. were widely used in the preparation of this work.

References

- Albrecht, A. & Skordis, C. 2000, *Phys. Rev. Lett.*, 84, 2076
- Amendola, L. 2000, *Phys. Rev. D*, 62, 043511
- Becker, R.H. et al., 2001, *AJ*, 122, 6

- Brax, P., Martin J. & Riazuelo A., 2000, Phys.Rev. D, 62, 103505
- Brax, P. & Martin, J., 1999, Phys.Lett., B468, 40
- Brax, P. & Martin, J., 2000, Phys.Rev. D, 61, 103502
- Bruscoli, M., Ferrara, A., & Scannapieco, E., 2002, MNRAS, 330, L43
- Carretti, E., et al., 2000, in: IAU Symposium 201, New Cosmological Data and the Value of Fundamental Parameters, Astron. Soc. Pacif. Conf. Series, eds. Lasenby A. and Wilkinson A.
- Colombo, L.P.L. & Bonometto, S.A., 2002, New Astr., in press, astro-ph/0209505
- Djorgovski, S.G., Castro, S.M., Stern, D. & Mahabal, A.A., 2001, ApJ, 560, L5
- Dolgov A.D., 2002, Invited Review Talk given at the VII Workshop on Topics in Astroparticle and Underground Physics (TAUP2001), Sept. 2001, L.N. Gran Sasso, Italy, astro-ph/0201107
- Efstathiou, G., et al., 2002, MNRAS, 330, L29
- Ferreira, P.G. & Joyce, M. 1998, Phys. Rev. D, 58, 023503
- Kovac C., Leitch E.M., Pryke C., Carlstrom J.E., Halverson N.W., Holzappel W.L. 2002, ApJ, in press, astro-ph/0209478
- Ma, C.P. & Bertshinger, E., 1995, ApJ, 455, 7
- Macculi, C., et al., 2000, in: What are the Prospect for Cosmic Physics in Italy?, eds. Aiello S. and Blanco A., Conf. Proc. 68, 171.
- Miralda-Escudé, J. 2002, ApJ, submitted, astro-ph/0211071
- Percival, W.J., et al. 2002, MNRAS, in press, astro-ph/0206256
- Perlmutter, S., et al. 1998, Nature 391, 51
- Perrotta, F. & Baccigalupi, C. 1999, Phys. Rev. D, 59, 123508
- Peverini et al., 2001, Int. Workshop on Background Polarized Emission, Bologna, 2001, AIP Conf Proc.
- Ratra, B. & Peebles P.J.E., 1988, Phys Rev D, 37, 3406
- Riess, A.G., et al 1998, AJ 116, 1009
- Steinhardt, P.J., Wang, L., & Zlatev, I. 1999, Phys. Rev. D, 59, 123504
- Stompor R. et al, 2001, ApJ, 561, L7
- Tucci, M., Carretti, E., Cecchini, S., Cortiglioni, S., Fabbri, R. & Pierpaoli, E., 2000, New Astr., 5, 181
- Wetterich, C., 1995, A & A, 301, 321
- Zaldarriaga, M., 1998, ApJ, 503
- Zlatev, I., Wang L. & Steinhardt P.J., 1999, Phys Rev Lett, 82, 896

Appendix A

Starting from the Lagrangian density for the ϕ field, self-interacting through a potential $V(\phi)$, and using Euler–Lagrange equations, we can work out the equations for the background unperturbed field ϕ and its fluctuations $\delta\phi$. The latter reads

$$\ddot{\delta\phi} + 2\frac{\dot{a}}{a}\dot{\delta\phi} + (k^2 + V''a^2)\delta\phi + \dot{\phi}\frac{\dot{h}}{2} = 0 \quad (\text{A1})$$

and we aim to show that this is equivalent to eq. (5.6), that we report here:

$$\theta + \frac{\dot{h}}{2} = -\frac{1}{1+w}[\dot{\delta} + 3\frac{\dot{a}}{a}(c_s^2 - w)\delta] . \quad (\text{A2})$$

An equation equivalent to eq. (A2) is given, for a generic fluid, by Ma & Bertschinger (1955), who derive it from the pseudo-conservation of the energy–momentum tensor T_{ij} .

In this Appendix, for the sake of simplicity, we omit the subscript $_{DE}$ to

$$\delta = \frac{\delta\rho_{DE}}{\rho_{DE}} \quad \text{and} \quad \theta = \frac{k^2}{a^2} \frac{\dot{\phi}\delta\phi}{\rho_{DE}(1+w)}, \quad (\text{A3})$$

as well as to the energy density ρ and to the pressure p of DE.

The proof is simpler if we start from eq. (A2) and obtain eq. (A1). Let us first multiply both sides of eq. (A2) by $(1+w)\rho$ and replace $\dot{\delta}$ by

$$\frac{\dot{\delta}\rho}{\rho} - \frac{\dot{\rho}\delta\rho}{\rho^2} = \frac{\dot{\delta}\rho}{\rho} + 3\frac{\dot{a}}{a}(1+w)\frac{\delta\rho}{\rho} . \quad (\text{A4})$$

In this way, we obtain

$$\rho(1+w)(\theta + \frac{\dot{h}}{2}) = -\dot{\delta}\rho - 3\frac{\dot{a}}{a}(1+c_s^2)\delta\rho . \quad (\text{A5})$$

Owing to the definition of θ (eq. A3) and thanks to the relation $(1+w)\rho = \rho + p = \dot{\phi}^2/a^2$, the l.h.s. of eq. (A5) becomes $(k^2/a^2)\dot{\phi}\delta\phi + (\dot{\phi}^2/a^2)(\dot{h}/2)$, while, at the r.h.s., we may replace $\delta\rho$ and $\dot{\delta}\rho$ with the expressions obtainable from the definition of $\rho = \dot{\phi}^2/2a^2 + V$. Both sides of the resulting equation must then be divided by $\dot{\phi}/a^2$, so obtaining

$$k^2\delta\phi + \dot{\phi}\frac{\dot{h}}{2} = -\dot{\delta}\phi - \left(\frac{\ddot{\phi}}{\dot{\phi}} + a^2\frac{V'}{\dot{\phi}} - 2\frac{\dot{a}}{a}\right)\delta\phi - V''a^2\delta\phi - 3\frac{\dot{a}}{a}(1+c_s^2)\left(\frac{\dot{\phi}\delta\phi}{a^2} + V'\delta\phi\right)\frac{a^2}{\dot{\phi}} . \quad (\text{A6})$$

Here we ought to use the equation of motion of the unperturbed field ϕ , which can be easily reset to yield that $\ddot{\phi}/\dot{\phi} = -2\dot{a}/a - a^2V'/\dot{\phi}$. Rearranging the

terms, we then obtain:

$$\ddot{\delta\phi} + 2\frac{\dot{a}}{a}\dot{\delta\phi} + (k^2 + V''a^2)\delta\phi + \dot{\phi}\frac{\dot{h}}{2} = 3\frac{\dot{a}}{a}[(1 - c_s^2)\dot{\delta\phi} - (1 + c_s^2)a^2\frac{V'}{\dot{\phi}}\delta\phi]. \quad (A7)$$

Eq. (A7) coincides with the equation of motion (A1), provided that the r.h.s. vanishes. This follows the very definition of sound velocity

$$c_s^2 = \frac{\delta p}{\delta\rho} = \frac{\dot{\phi}\dot{\delta\phi}/a^2 - V'\delta\phi}{\dot{\phi}\dot{\delta\phi}/a^2 + V'\delta\phi} \quad (A8)$$

from which we easily obtain that $(1 + c_s^2)/(1 - c_s^2) = \dot{\phi}\dot{\delta\phi}/a^2V'\delta\phi$. This last relation clearly yields the vanishing of the r.h.s. of eq. (A7).

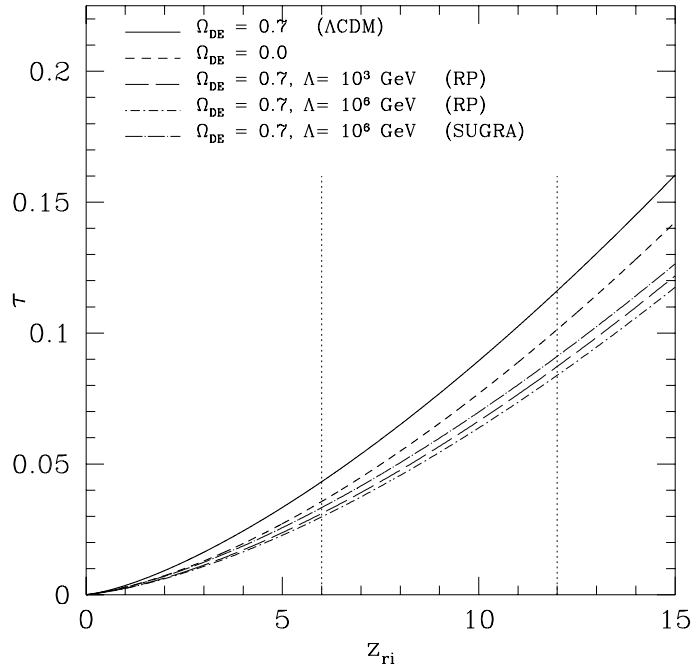


Fig. 1. Optical depth to CMB photons, in different models with $\Omega_m = 0.3$, $h = 0.7$ and $\Omega_b h^2 = 0.02$, as a function of the reionization redshift z_{ri} . The most likely interval for z_{ri} is comprised between the two vertical dotted lines.

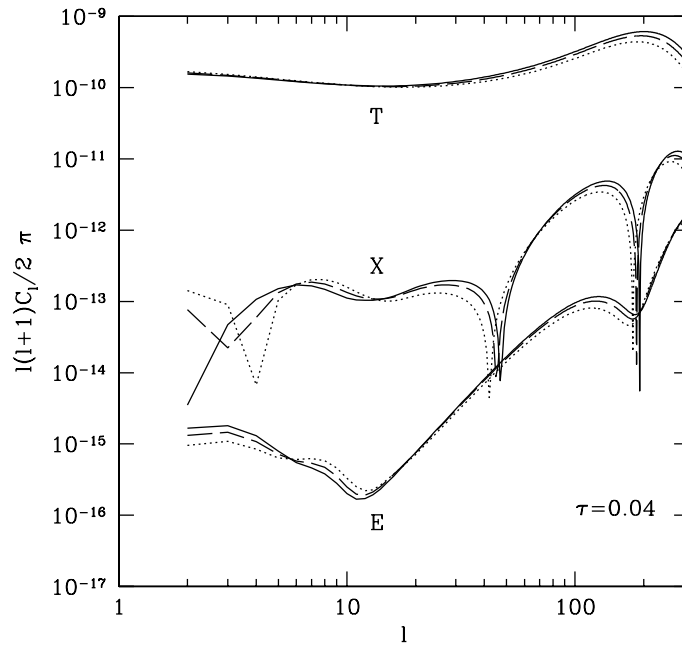


Fig. 2. Angular spectra of RP models with $\tau = 0.04$. Continuous (dashed, dotted) lines correspond to $\Lambda = 10^3$ ($10^6, 10^9$) GeV. The absolute values of C_l^X is plotted; changes of sign are indicated by cusps; notice such cusps at low l .

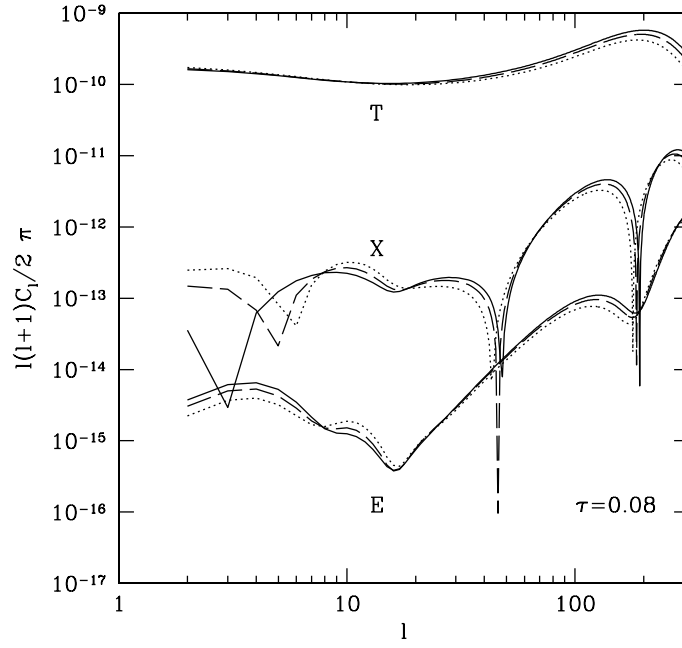


Fig. 3. As Fig. 2, but for $\tau = 0.08$.

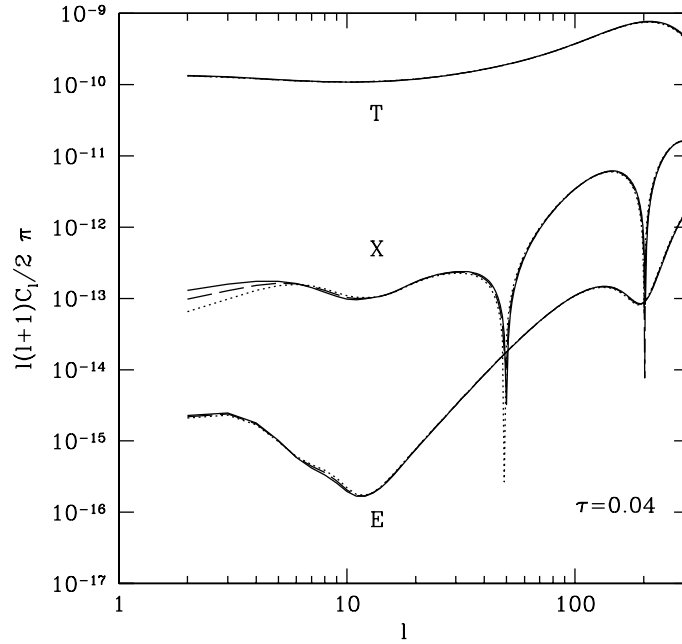


Fig. 4. As Fig. 2, but for SUGRA potentials. Although the only significant difference among SUGRA spectra concerns C_l^X at quite low l , it is noticeable how more significant differences were among RP potentials.

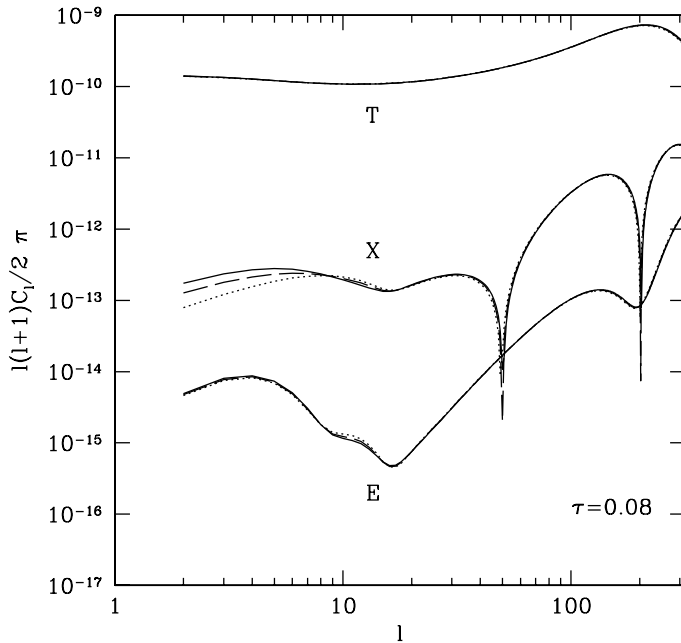


Fig. 5. As Fig. 4, but for $\tau = 0.08$.

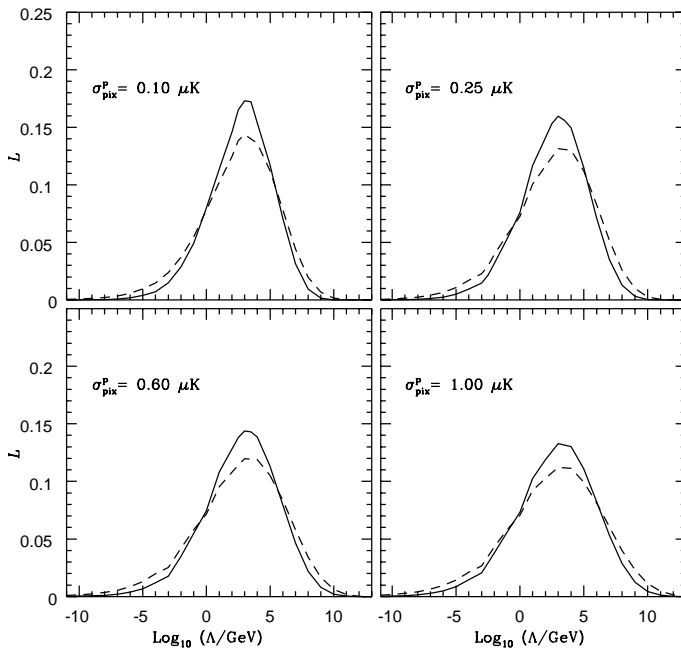


Fig. 6. Average likelihood of Λ values, for a RP potential with $\Lambda = 10^3 \text{ GeV}$. Continuous (dashed) lines refer to $\tau = 0.08$ (0.04). Notice that models with $\Lambda < 1$ are indistinguishable from ΛCDM . Accordingly, even with $\sigma_{pix}^P \simeq 0.1 \mu\text{K}$, there is a large fraction of realizations for which the model cannot be distinguished from ΛCDM ; such fraction is specified in Figs. 13 to 15.

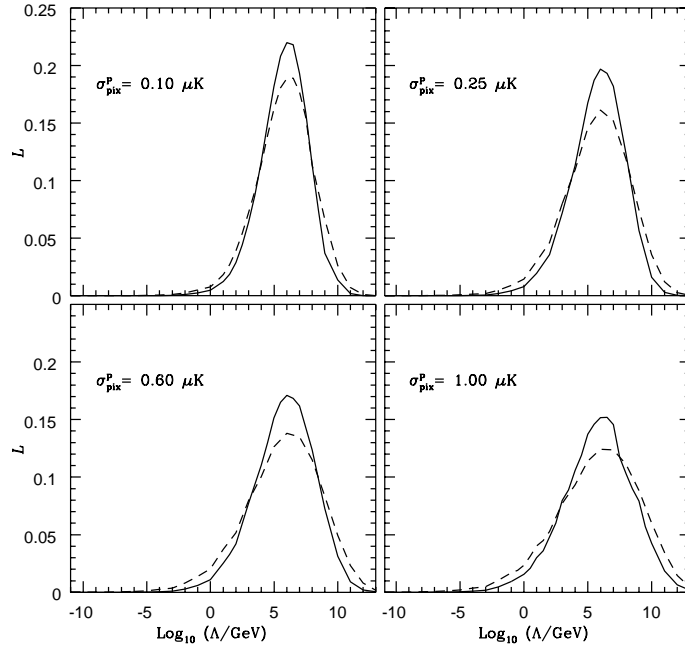


Fig. 7. The same as Fig. 6, but for $\Lambda = 10^6$. Such model is in marginal agreement with data on SNIa.

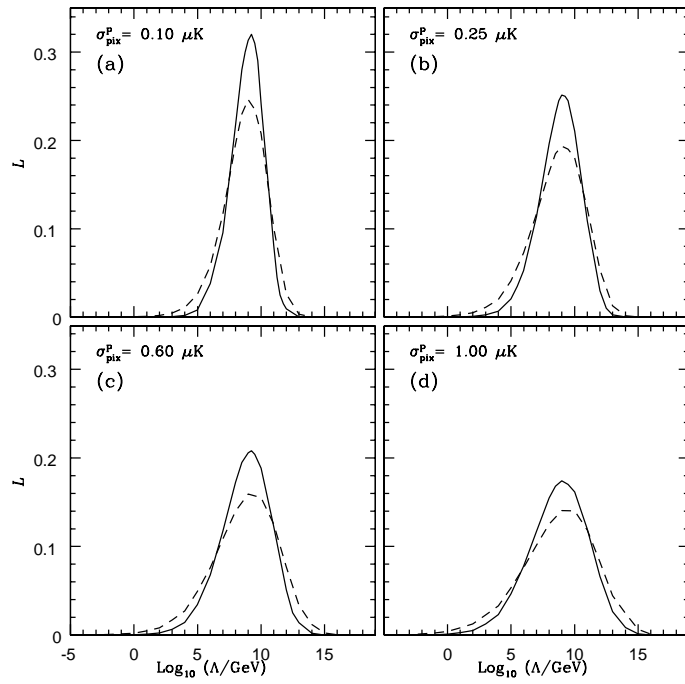


Fig. 8. The same as Fig. 6, but for $\Lambda = 10^9$.

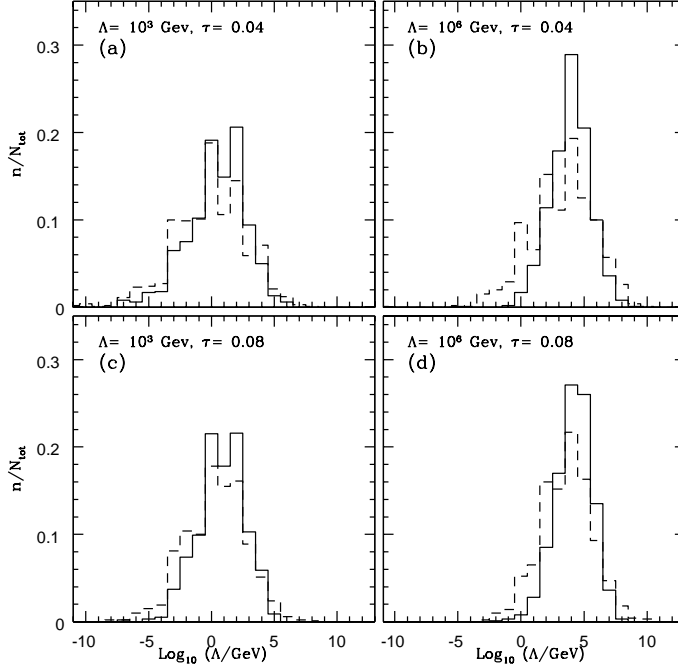


Fig. 9. Distribution of $1\text{-}\sigma$ lower limits on Λ . The continuous (dashed) curve refer to $\sigma_{pix}^P = 0.1$ (1) μK . Notice that, even in the worst case, there is a substantial fraction of realizations which allow to distinguish RP from ΛCDM . For $\Lambda = 10^6\text{GeV}$ and $\tau = 0.08$, the fraction of realizations indistinguishable from ΛCDM , with the reasonable noise level $\sigma_{pix}^P = 1 \mu\text{K}$, is $\sim 2\%$.

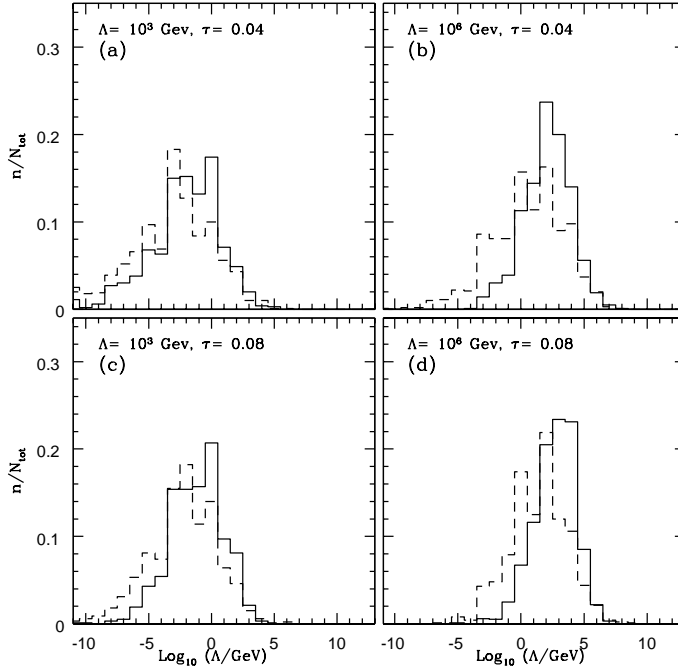


Fig. 10. As Fig. 9, at the $2\text{-}\sigma$ confidence level. For $\Lambda = 10^6\text{GeV}$ and $\tau = 0.08$, the fraction of realizations indistinguishable from ΛCDM , with $\sigma_{pix}^P = 1 \mu\text{K}$, is $\sim 16\%$.

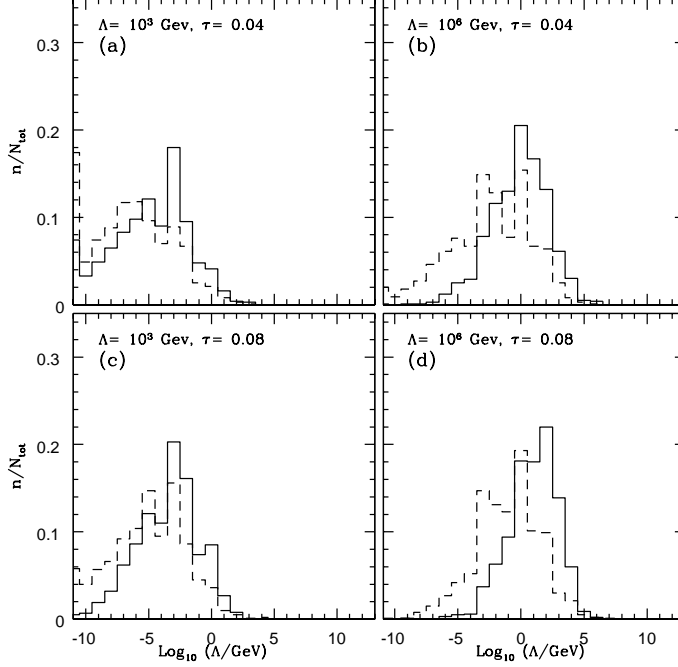


Fig. 11. As Fig. 9, at the $3\text{-}\sigma$ confidence level. For $\Lambda = 10^6\text{GeV}$ and $\tau = 0.08$, the fraction of realizations indistinguishable from ΛCDM , with $\sigma_{pix}^P = 1\mu\text{K}$, is more than 50%; this however means that, in more than 1/3 of realizations, even with $\sigma_{pix}^P = 1\mu\text{K}$, there is the possibility to distinguish a RP model from ΛCDM at the $3\text{-}\sigma$ level.

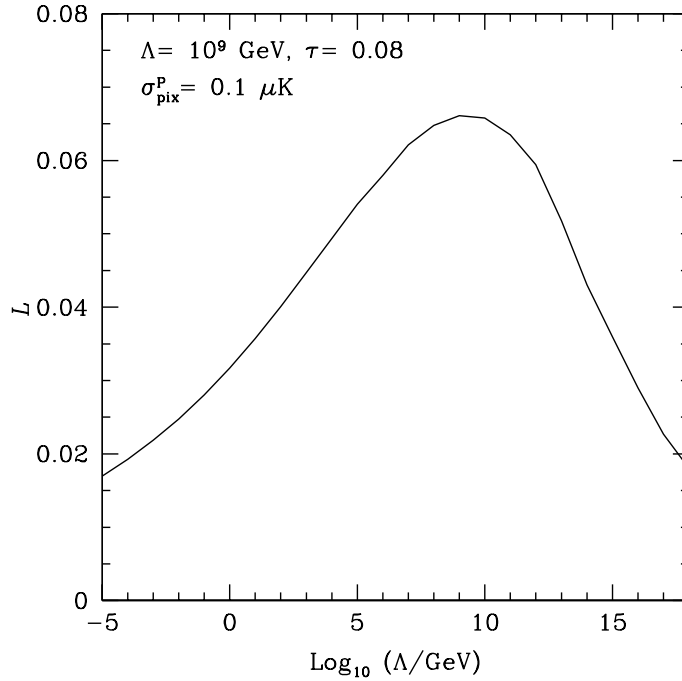


Fig. 12. This figure is analogous to Fig. 6, but concerns a SUGRA model with $\Lambda = 10^9\text{GeV}$ and $\tau = 0.08$.

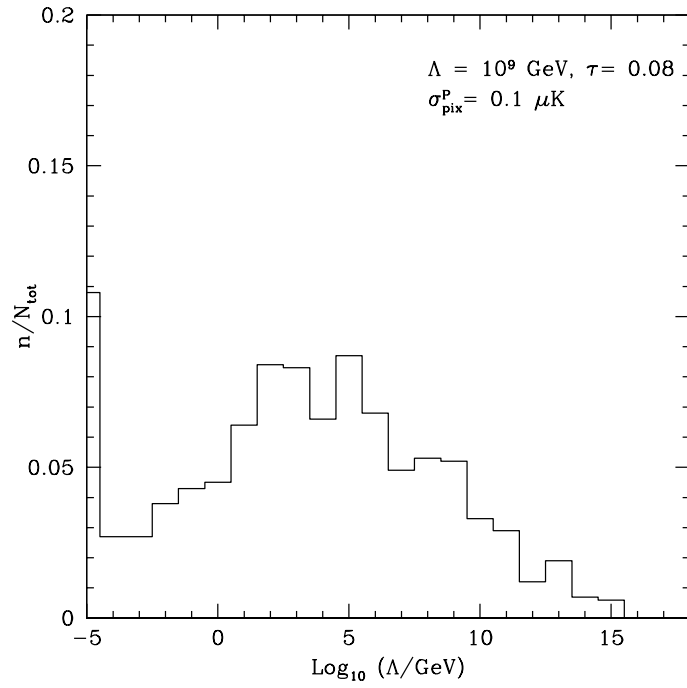


Fig. 13. $1\text{-}\sigma$ lower limit distribution for SUGRA with $\Lambda = 10^9 \text{ GeV}$.

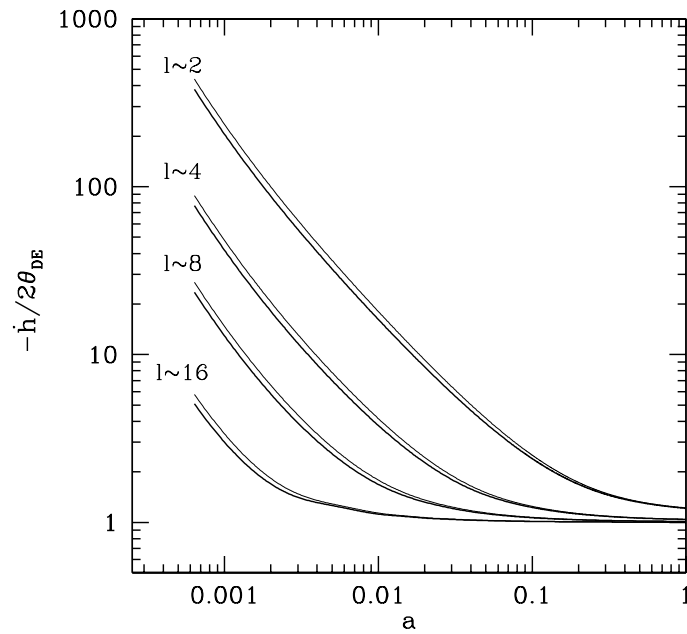


Fig. 14. The ratio $-\dot{h}/2\theta_{DE}$ is plotted with a thick (thin) line for RP models with $\Lambda = 10^3(10^6)\text{GeV}$